Open Access

Prediction and Experimental Study of the Acoustic Soundproofing Windows Using a Parallelepiped SVU

HuyQuang Nguyen[*,1], Takashima Yusuke[2], Nishimura Yuya[3], Nishimura Sohei[3], Nishimura Tsuyoshi[2] and Yano Takashi[1]

[1]*Graduate School of Science and Technology, Kumamoto University, 2-39-1 Kurokami Kumamoto, Japan*

[2]*Faculty of Computer Science, Sojo University, 4-22-1 Ikeda Kumamoto, Japan*

[3]*Kumamoto National College of Technology, 26-27 Hirayama Shinmachi Yatsushiro, Japan*

Abstract: A conceptual model for window manufacturing which is capable of ventilation, regulating sunlight, and reducing a traffic and environment noise has been presented in previous studies. This window combines two basic components: a soundproofing ventilation unit (SVU) and a lighting unit. The former is constructed using a rectangular cubic with input and output openings at both ends. However, when using the rectangular cubic, the indoor lighting effect could not be expected to be as great. This paper deals with a parallelepiped shape and those acoustic characteristics based on the experiments and comparisons with those of rectangular cubic SVU.

Keywords: Soundproofing, ventilation unit, parallelepiped.

1. INTRODUCTION

In developing countries, many environmental issues were caused due to the backward and inefficient management and policies that could not keep up with the speed of the booming development in various fields such as the economy, transportation and society. The traditional production method in those countries is the combination of small-scaled production facilities and accommodation in village houses. Recently, under the effect of the industrialization process, labor methods and scales have changed, creating an industrial zone in those residential areas. This fact is leading to the growth of a new type of pollution, namely, industrial noise.

The authors have presented a concept for windows which are capable of ventilation, and preventing environment noise for developing tropical countries [1]. This window combines two basic components: the soundproofing ventilation unit (SVU) and the lighting unit. The SVU is constructed using a rectangular cubic with input and output opening at both ends. However, when using the rectangular cubic SVU, the indoor lighting effect could not be expected to be as great. Accordingly, to increase the amount of light, meaning the sun's rays can be projected into the room as much as possible, there is a need to change SVU with a shape other than the rectangular cubic.

Due to the fact that SVU must have a large volume to attenuate the low frequency noise, many resonances of the higher-order mode waves will be generated inside the unit [2-5]. Consequently, in order to have a great soundproofing effect, it is necessary to take into consideration the dimension and placement of input and output openings in such a way that would minimize the effects of the higher-order mode. Needless to say, a more important selection is the shape of SVU.

This paper deals with a parallelepiped SVU and those acoustic characteristics based on the experiment and comparison with those of rectangular SVU.

2. DESIGN OF SOUNDPROOFING WINDOWS AND THE IMPROVEMENT OF LIGHTING EFFECT

Casement windows are a dominant type of common house windows in tropical countries. The structure of a window that can swing around on hinges and that has ventilation slits enables the window to adapt to lighting and ventilation demand for wide variety of activities during the day and night time. The most important advantage of using ventilation slits is to allow ventilation even when the windows are closed to exclude inclement weather. Nevertheless, the growing level of industrial noise exposure inside living quarters makes these windows unsuitable when sound isolation becomes an emergency requirement.

In that context, we propose a new model of casement door and windows which can allow ventilation and has soundproofing abilities. The structure of our proposed windows model has been reported in previous papers [1]. It combines two basic components: ventilation and lighting as shown in Fig. (**1**). The lighting unit can be constructed using one or two glass layers which are mounted between two rectangular ventilation components with input and output openings. The unit requires a simple internal structure and a large input and output to maximize ventilation as well as to prevent outside noise from entering the home. The

*Address correspondence to this author at the Graduate School of Science and Technology, Kumamoto University, 2-39-1 Kurokami Kumamoto, Japan; Tel: +81-96-342-3013; Fax: +81-96-342-3010;
E-mail: nhuyquang@yahoo.com

1874-8376/12 2012 Bentham Open

effectiveness of the soundproofing of this design has been proven in published papers [1]. Nonetheless, given the concern about the efficiency of lighting, this window has a defect that needs to be improved.

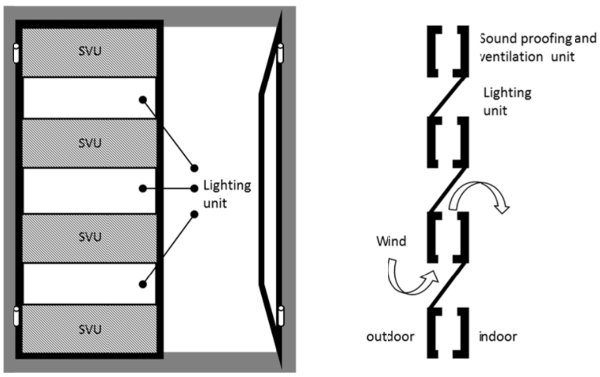

Fig. (1). Design of soundproofing casement windows.

Since the sun's rays are oblique almost all the time, a perpendicular shape of the SVU will prevent a large amount of light rays from reaching the glass layer of the lighting unit. Our task is to maximize the area of the surface at which the sun's rays can be received. In order to meet that demand, the shape of SVU should be oblique at the angle that can fit well to the direction of the sun's rays. This concept suggests a new design of the SVU in the form of an oblique parallelepiped as shown in Fig. (**2**). The parallelepiped SVU is described in detail in Fig. (**3**) with the θ as an oblique angle between the vertical axis and the sun's rays. The difference in the acoustic characteristics of parallelepiped SVU from the rectangular one will be explained.

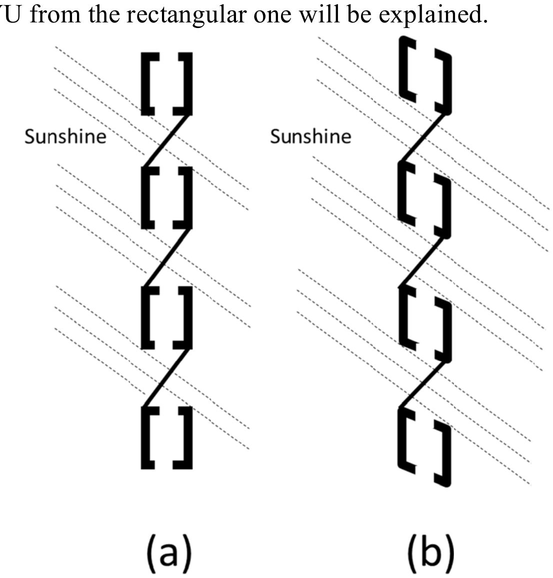

Fig. (2). Improvement of lighting effect by using a parallelepiped SVU.

3. METHOD OF ANALYSIS

In order to achieve a high soundproofing effect, we need to find out the resonance mechanism and the resonance frequency according to the shape of the SVU. Hereinafter, we will summarize some analysis methods used for the study of the rectangular SVU.

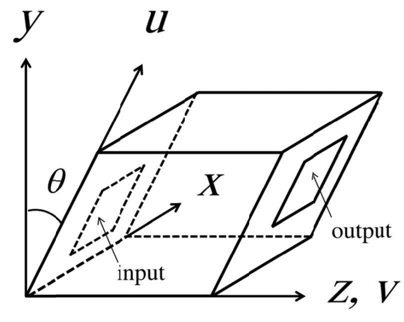

Fig. (3). Parallelepiped SVU and it's coordinates.

3.1. Insertion Loss

Acoustic characteristics of an acoustic element which has a length L and section area S can be described by the four-pole parameters A, B, C and D as [6]

$$\begin{bmatrix} P_1 \\ U_1 \end{bmatrix} = \begin{bmatrix} A & B \\ C & D \end{bmatrix} \begin{bmatrix} P_2 \\ U_2 \end{bmatrix} = \begin{bmatrix} \cos kl & jZ\sin kl \\ j\frac{1}{Z}\sin kl & \cos kl \end{bmatrix} \begin{bmatrix} P_2 \\ U_2 \end{bmatrix} \quad (1)$$

where P_1 and U_1 are the sound pressure and velocity at the input, P_2 and U_2 are those at the output, ρ is the quiescent gas pressure, c is sound velocity and k is wave number. When this element is connected to the source, their performance can be expressed through the use of insertion loss IL defined by [6]

$$IL = 10\ log\frac{W_r}{W_0} = 10\ log\left|\frac{U_1}{U_2}\right|^2 \quad (2)$$

Here, W_r and W_0 are the radiated powers at one point in space with or without the acoustic element inserted between that point and the source. The ratio of U_1/U_2 is equal to the D parameter of (1), as far as the constant velocity source is concerned.

When the acoustic element is connected in a series as shown in Fig. (**4**), and when the sectional area of elements 1 and 3 are sufficiently small to compare with those of element 2, and the D parameter of the whole system can be described by the following approximated equation:

$$D = (\cos kl_1)\,(C_w)\,(jZ_3 \sin kl_3) \quad (3)$$

where C_w denotes the C parameter of element 2. As shown in (2) and (3), in order to obtain a reliable IL effect, D parameter must be high enough. In other words, the design of element 2 that has a high value of C_w is demanded.

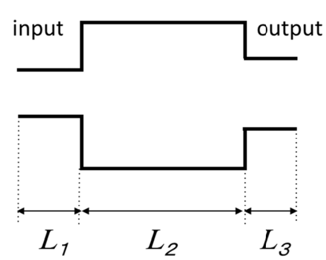

Fig. (4). Basic structure of acoustic system.

3.2. Computation of C_w

We found the sound pressure on the input and output of the rectangular SVU as shown in Fig. (**5**). The input and output have a sectional area of S_i and S_L, respectively.

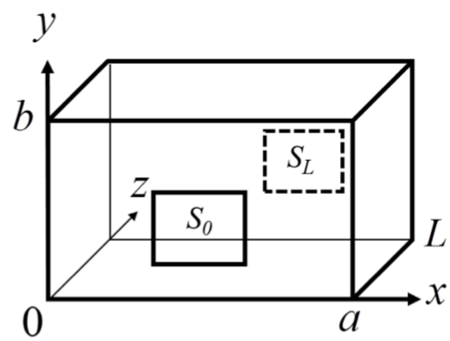

Fig. (5). Computation model of SVU.

The completion of the wave-equation in terms of the velocity potential ϕ when expressed in rectangular coodinates is given by [1]

$$\phi = \left(Ae^{\mu z} + Be^{-\mu z} \right)\left(C\sin\alpha x + D\cos\alpha x \right). \left(E\sin\sqrt{s^2-\alpha^2}\,y + F\cos\sqrt{s^2-\alpha^2}\,y \right) \tag{4}$$

where A, B, C, D, E and F are arbitrary constants determinable from the boundary conditions, α, s and μ are constants.

$V_x = -\partial\phi\,/\,\partial x$, $V_y = -\partial\phi\,/\,\partial y$ and $V_z = -\partial\phi\,/\,\partial z$ are the velocity components in the x, y and z directions, respectively. Assuming the walls of the cavity are perfectly rigid and the loss at the wall can be neglected, the boundary conditions are

[1] at $x = 0,\ V_x = 0$ (5)

[2] at $x = a,\ V_x = 0$ (6)

[3] at $y = 0,\ V_y = 0$ (7)

[4] at $y = b,\ V_y = 0$ (8)

[5] at $z = 0,\ V_z = V_0\ F_0(x,y)$ (9)

[6] at $z = L,\ V_z = V_L\ F_L(x,y)$. (10)

where V_0 and V_L are the driving velocities at the input and output, $F_0(x,y)$=1 at the input and $F_0(x,y)$=0 elsewhere, $F_L(x,y)$=1 at the output and $F_L(x,y)$=0 elsewhere.

Based on the above boundary conditions, the velocity potential ϕ and the sound pressure defined by $P = jk\rho c\phi$ can be determined. Therefore the sound pressure acting on an output can be expressed in term

$$P_L = jkZ_w\left[S_w \sum_{m=0}^{\infty}\sum_{n=0}^{\infty}\left\{ \frac{1}{\mu_{m,n}\sinh\left(\mu_{m,n}L\right)}U_0\,D^a_{m,n} + \frac{\cosh\left(\mu_{m,n}L\right)}{\mu_{m,n}\sinh\left(\mu_{m,n}L\right)}U_L\,D^b_{m,n} \right\} \cos\left(\frac{m\pi x}{a}\right)\cos\left(\frac{n\pi y}{b}\right) \right] \tag{11}$$

where

$$\mu_{m,n} = \sqrt{\left(m\pi/a\right)^2 + \left(n\pi/b\right)^2 - k^2} \tag{12}$$

$U_0 = V_0\,S_0$ is the volume velocity at input

$U_L = V_L\,S_L$ is the volume velocity at input

$Z_w = \rho c\,/\,S_w$ is the characteristic acoustic impedance of the cavity

$D^q_{m,n}$ are the sound levels corresponding to (m, n) higher-order mode

$\dot{\sum}$ means $\sum_{m=0}^{\infty}\sum_{n=0}^{\infty}$ without the cases of m=n=0.

The average sound pressure acting on the output can be found as

$$\bar{P}_L = \frac{1}{S_L}\iint_{S_L} P_L\,dx\,dy$$

$$= jZ_w\left\{ -\frac{U_0 - U_L\cos(kL)}{\sin(kL)} + \sum_{m=1}^{\infty}\left[\frac{\bar{Q}^a_{m,0}\,U_0}{\mu_{m,0}\sinh\left(\mu_{m,0}L\right)} + \frac{\cosh\left(\mu_{m,0}L\right)\bar{Q}^b_{m,0}\,U_L}{\mu_{m,0}\sinh\left(\mu_{m,0}L\right)} \right] + \sum_{n=1}^{\infty}\left[\frac{\bar{Q}^a_{0,n}\,U_0}{\mu_{0,n}\sinh\left(\mu_{0,n}L\right)} + \frac{\cosh\left(\mu_{0,n}L\right)\bar{Q}^b_{0,n}\,U_L}{\mu_{0,n}\sinh\left(\mu_{0,n}L\right)} \right] + \dot{\sum}\left[\frac{\bar{Q}^a_{m,n}\,U_0}{\mu_{m,n}\sinh\left(\mu_{m,n}L\right)} + \frac{\cosh\left(\mu_{m,n}L\right)\bar{Q}^b_{m,n}\,U_L}{\mu_{0,n}\sinh\left(\mu_{m,n}L\right)} \right] \right\} \tag{13}$$

in which $\bar{Q}^q_{m,n}$ is the average sound level corresponding to (m, n) higher-order mode

The first term on the bracket of (13) represents the sound pressure of the plane wave that propagates in the z axis and the second one represents the sound pressure components of higher order mode wave, respectively.

The C_w can be obtain by $C_w = U_0 / \bar{P}_L$ while U_L=0, namely

$$C_w = \left.\frac{U_0}{\bar{P}_L}\right|_{U_L=0}$$

$$= \frac{1}{-\frac{1}{\sin(kL)} + \sum_{m=1}^{\infty} \frac{\bar{Q}^a_{m,0}}{\mu_{m,0}\sinh(\mu_{m,0}L)} + \sum_{n=1}^{\infty} \frac{\bar{Q}^a_{0,n}}{\mu_{0,n}\sinh(\mu_{0,n}L)} + \sum \frac{\bar{Q}^a_{m,n}}{\mu_{m,n}\sinh(\mu_{m,n}L)}} \quad (14)$$

4. METHOD OF MEASUREMENT

4.1. Measurement of C_w

The measurement apparatus as shown in Fig. (**6**) was used to measure the value of C_w. Two microphones were located at both sides of the cavity to measure the sound pressure P_A and P_B, respectively. The relationship between them is given by

$$\begin{pmatrix} P_A \\ U_A \end{pmatrix} = \begin{pmatrix} \cos(kL_0) & jZ_0\sin(kL_0) \\ j\frac{1}{Z_0}\sin(kL_0) & \cos(kL_0) \end{pmatrix} \begin{pmatrix} A_w & B_w \\ C_w & D_w \end{pmatrix} \begin{pmatrix} P_B \\ U_B \end{pmatrix} \quad (15)$$

where the first term on the right side represents the four-pole parameters of the input pipe which has in length L_0 and the second one represents those of a cavity. Symbol U_A, U_B and Z_0 represent a volume velocity and acoustic impedance of the inlet pipe, respectively. By installing the microphone 2 on the output, U_B will become zero thus (15) can be obtained as

$$20\log_{10}|C_w| = 20\log_{10}|P_A / P_B| - 20\log_{10}|Z_0\sin(kL_0)| \quad (16)$$

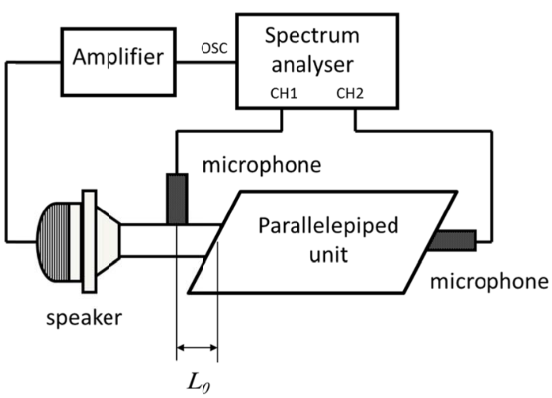

Fig. (6). Block diagram of the experimental apparatus.

It can be seen that C_w can be found by subtracting the acoustic characteristic of inlet pipe from the measured results of sound pressure P_A and P_B.

4.2. Measurement Using Reverberation Chambers

An experiment was conducted using the reverberation chamber method to verify the actual sound attenuation characteristics. Fig. (**7**) shows the experimental setup. The volumes of reverberation chambers are 98m^3 and 179 m^3. The rectangular and parallelepiped SVU are installed at the aperture by a casing composed of a plank. The sound source is a loudspeaker fed by pink noise, and five microphones located in each chamber measure the spatially averaged sound pressure. The pressure levels in the sending chamber were 100 -105 dB to achieved pressure level of 70 - 80 dB in the receiving room. The actual sound attenuation of SVU will be estimated by the difference from the measurement results with and without SVU inserted between two reverberation chambers.

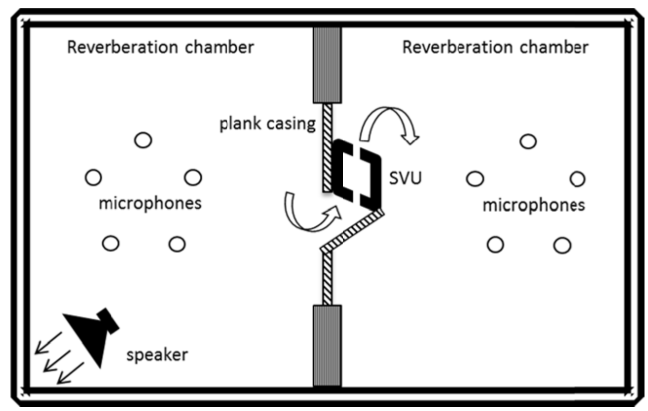

Fig. (7). Measurement system based on the reverberation chamber method.

5. RESULTS AND DISCUSSIONS

At first, let us consider a generation mechanism of higher-order mode sound pressure component in the case of rectangular SVU. C_w is defined by (14) including the output sound pressure $\bar{P}_L$ at its denominator. In order to obtain an IL effectively C_w must be at great, in other words, low level of $\bar{P}_L$ is preferable. Referring to (14), $\bar{P}_L$ becomes great when its denominator sin(kL) and $\mu_{m,n}$ sinh ($\mu_{m,n}L$) sinh are zero, namely, at the following resonance frequencies of

$$\sin(kL) = 0 \quad \therefore \quad f_0 = \eta\frac{c}{2L} \quad (\eta = 1, 2, 3....) \quad (17)$$

$$\mu_{m,n}\sinh(\mu_{m,n}L) = 0 \quad \therefore \quad f_{m,n} = \frac{c}{2\pi}\sqrt{\left(\frac{m\pi}{a}\right)^2 + \left(\frac{n\pi}{b}\right)^2 - \left(\frac{\eta\pi}{L}\right)^2} \quad (\eta = 0, 1, 2, 3....) \quad (18)$$

in which f_0 represents the resonance frequencies of the plane wave and $f_{m,n}$ represents those of higher-order mode. The first resonance frequencies of $f_{m,n}$ when η=0 which occur sequentially, are shown in an example of Fig. (**8**) when the dimensions of the rectangular SVU are a=0.48m, b=0.075m and L=0.29m, respectively. The generally, at the frequency range where the higher-order mode waves are generated, the sound pressure $\bar{P}_L$ will increase and when the resonance frequencies of other modes co-occur, C_w will be small and the *IL* can not be expected to be as great. The generation mechanism of these frequencies can be understood according to the calculation example shown in Fig. (**9a**) with (2,0) and (4,0) modes.

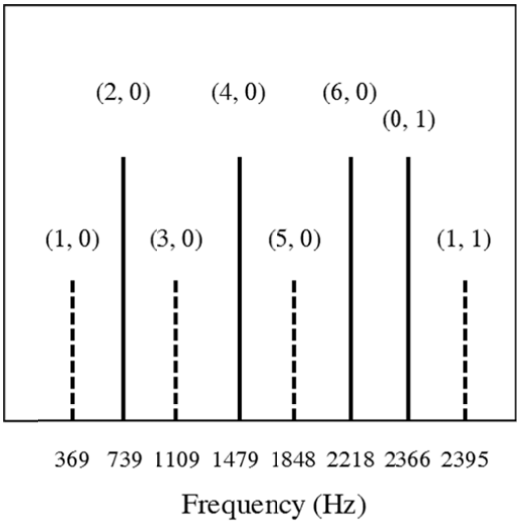

Fig. (8). The first resonance frequencies of some (m, n) modes appear at the output of rectangular SVU. Dotted line and solid line represent the odd and even mode of m. Dimensions of SVU are a=0.48cm, b=0.075cm and L=0.29m.

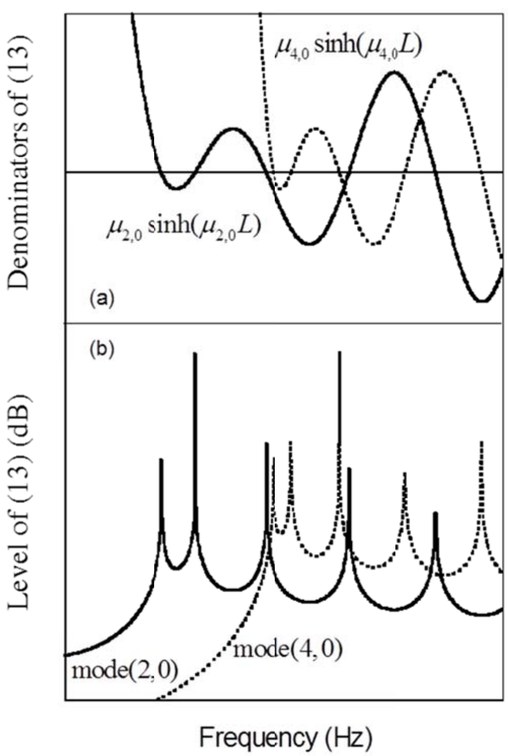

Fig. (9). Physical meaning (13). (**a**) Calculated example of (13) with (2, 0) and (4, 0) mode. (**b**) Spectrum of with (2, 0) and (4, 0) modes and their sum in solid line.

The sound pressure level of those wave components in dB are shown in Fig. (**9b**). They also have many resonance frequencies occur corresponding to the increasing of η in (18). Therefore, it is clear that when we eliminate an arbitrary higher-order wave mode by any method, we will not only avoid many resonances generated by this mode but also obtain the low level of the entire output sound pressure.

The measurement result of C_w, based on the method described in section 4-1, when the input and output are located in the center position is shown in Fig. (**10a**) while the denominators of (13) are shown in Fig. (**8a**). Note that, by locating the input or output at $x=a/2$ and $y=b/2$, $\cos(m\pi x/a)\cos(n\pi y/b)$ in (11) will become $\cos(m\pi/2)\cos(n\pi/2)$ and as a result, the (m, n) mode sound pressure does not appear when m=1, 3, 5 … for all values of n and when n=1, 3, 5 …. for all values of m. Therefore, as shown in Fig. (**10b**), the (m, n) mode sound pressure appears in SVU in the order of (2, 0), (4, 0) and so on.

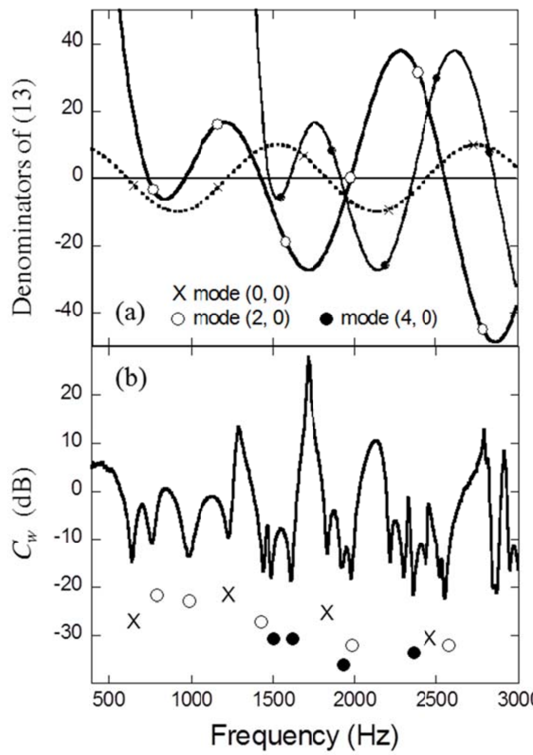

Fig. (10). Resonance frequencies of rectangular SVU. (**a**) Calculated result of the denominator of (13). (**b**) Measured result. Dimensions of SVU are a=0.48cm, b=0.075cm and L=0.29m.

Next, based on the analytical and measured results as mentioned above, let us consider the case when using a parallelepiped SVU.

An experiment was performed with two parallelepiped SVU of the same dimensions with rectangular SVU (a=48cm, b=7.5cm, L=29cm). The external angle θ is 45^0 and 60^0, respectively. Fig. (**11**) shows the difference of C_w between parallelepiped SVU ($\theta = 60^0$) and rectangular SVU ($\theta = 0^0$). Symbol × represents the resonance frequencies of the plane wave, symbol O and ● are those of higher order modes when m=2, n=0 and m=4, n=0 in case of rectangular SVU as mentioned in Fig. (**10**). It can be found that the fundamental resonance frequencies of parallelepiped SVU are shifted to the low frequency range in comparison with those of rectangular SVU. Moreover, by the shift of these resonance frequencies C_w is widely different from those of rectangular SVU. This characteristic also appeared in the high frequency range as shown in Fig. (**12**). However, we may consider that although there are some discrepancies between both acoustic characteristics, C_w did not change significantly in wide frequency range. Fig. (**13**) shows the difference of C_w between parallelepiped SVU ($\theta = 45^0$) and rectangular SVU. The shift of resonance frequencies and varies of C_w are smaller in comparison with Fig. (**11**). Discrepancies of C_w depend on the change of external angle is shown in Fig. (**14**).

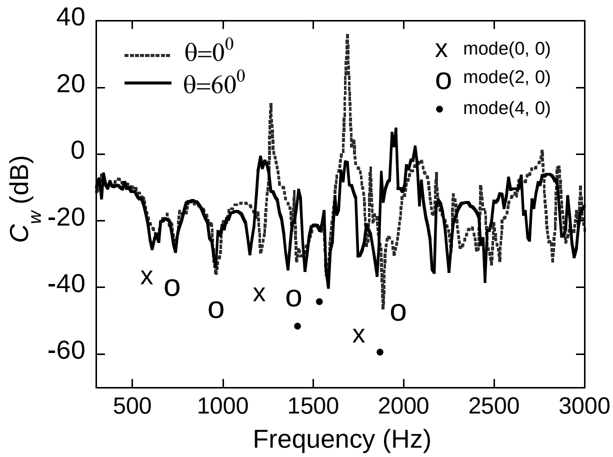

Fig. (11). Measured results of C_w. Solid line is parallelepiped SVU and dotted line is rectangular. Dimensions of SVU are a=0.48cm, b=0.075cm and L=0.29m.

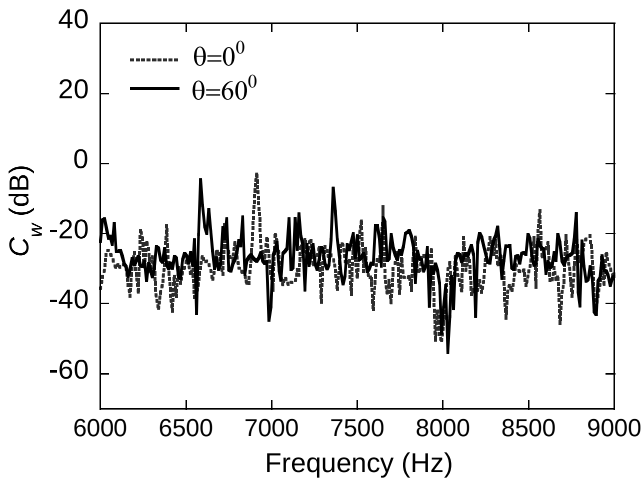

Fig. (12). Measured results of C_w in the frequency range of 6000Hz - 9000Hz. Solid line is parallelepiped SVU and dotted line is rectangular one.

Next, in order to verify the actual sound attenuation characteristics of parallelepiped SVU and comparing with those of rectangular SVU, experiments were conducted using the reverberation chamber method as mentioned in section 4.2. The same dimension of SVU (a=48cm, b=7.5cm, L=29cm) with openings of input and output were used in the experiments. Fig. (**15**) shows the measured results of both SVU when using an input and output having a shape as shown inside of the figure. The ratio of cross section area between SVU and input, output is 0.25. Attenuation in dB were obtained from the difference of the measurement results with and without SVU inserted between two reverberation chambers. Fig. (**16**) shows the measured results of parallelepiped SVU with the changing of an external angle. The sound propagating through SVU is a combination of plane wave and higher-order mode waves. Thus, a selection of input and output shapes that minimize those wave components as much as possible is very important. When we selected the input and output shape as shown in Figs. (**15**, **16**), many higher order mode wave resonances could be eliminated. However, (2, 0) and (4, 0) modes could not be eliminated. Based on the theoretical analysis of rectangular SVU, the soundproofing effect can be expected to be as high when suitable shape for the output is selected as shown in Fig. (**17**). The same soundproofing effect for parallelepiped SVU is confirmed from the measured results as shown in Fig. (**18**).

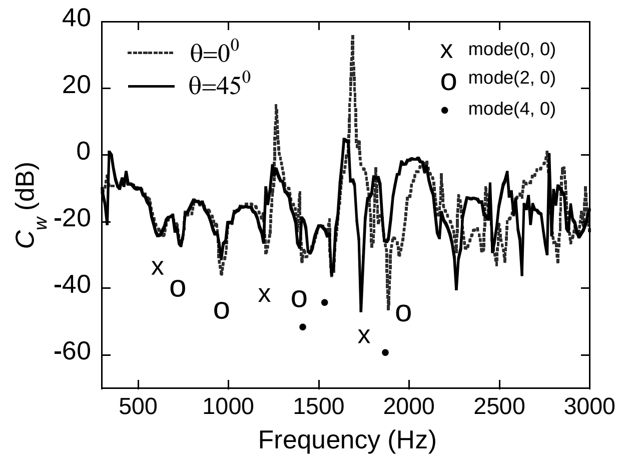

Fig. (13). Measured results of C_w. Solid line is parallelepiped SVU and dotted line is rectangular.

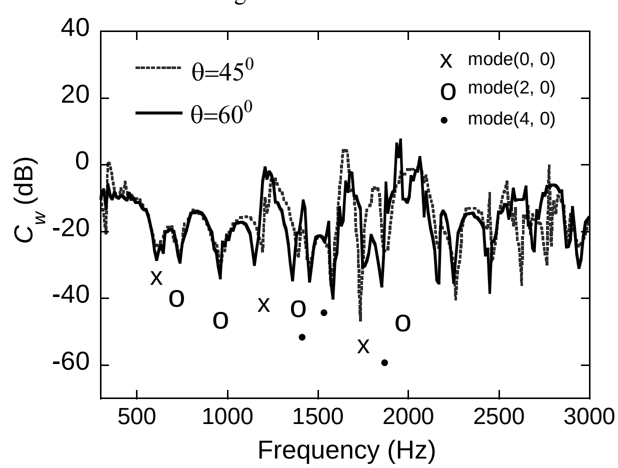

Fig. (14). Measured results of C_w with $\theta=45^0$ and 60^0.

From the above discussion based on the measured results, we may conclude that although there are some discrepancies on the resonance frequency and C_w level, the acoustic characteristics of parallelepiped SVU can be considered as similar with those of rectangular ones. Therefore, the soundproofing techniques of rectangular SVU can be applicable for parallelepiped SVU in practical use. In the

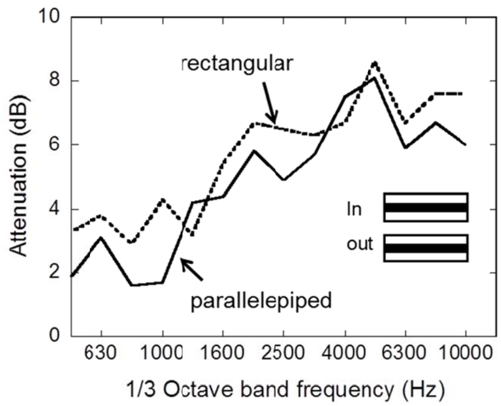

Fig. (15). Measured results of parallelepiped and rectangular SVU based on reverberation chamber method. Dimensions of SVU are a=0.48cm, b=0.075cm and L=0.29m.

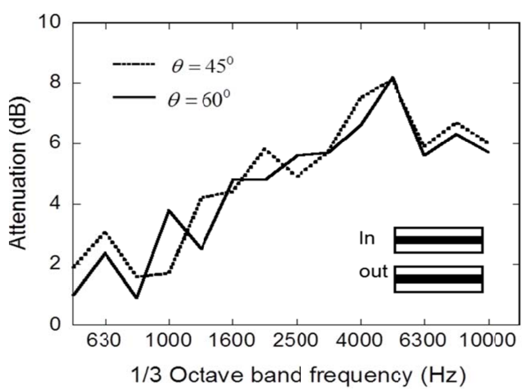

Fig. (16). Measured results of parallelepiped SVU with change of external angle based on reverberation chamber method.

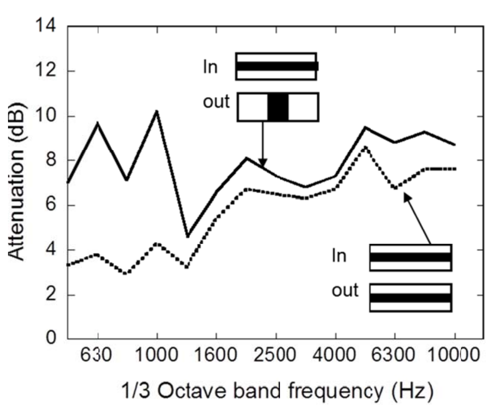

Fig. (17). Measured results of rectangular SVU with change of inputshape based on reverberation chamber method.

case where the theoretical calculation of parallelepiped SVU is required, it may use a analysis method as described in Appendix.

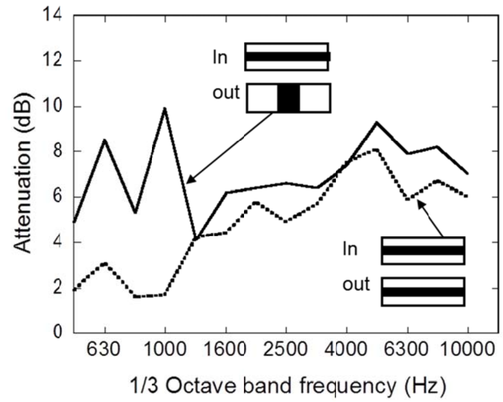

Fig. (18). Measured results of parallelepiped SVU with change of input shape based on reverberation chamber method.

CONCLUSIONS

Acoustic characteristics of the parallelepiped SVU were estimated by the comparison with those of rectangular ones. From the results obtained by measurement based on insertion-loss and reverberation chamber method, we may conclude that although there are some discrepancies on the resonance frequency and C_w level, the acoustic characteristic of parallelepiped SVU can be considered as similar with those of rectangular ones. Therefore, the soundproofing techniques of rectangular SVU can be applicable for parallelepiped SVU in practical use.

In order to maximize the soundproofing capability, it is necessary to minimize the effect of the plane wave sound pressure component. Moreover, it is necesssary to use sound absorbent material effective with current noise pollution inside the SVU. This technology will be present in an upcoming report.

ACKNOWLEDGEMENT

None declared.

CONFLICT OF INTEREST

None declared.

APPENDIX

Computation of C_w in the Case of Parallelepiped SVU

Wave equation in term of velocity potential is given by

$$\left(\frac{\partial^2}{\partial x^2}+\frac{\partial^2}{\partial y^2}+\frac{\partial^2}{\partial z^2}\right)\Phi=\frac{1}{c^2}\frac{\partial^2\Phi}{\partial t^2} \quad \text{(A-1)}$$

By using the relationship between Cartesian coordinate and Oblique one as shown in Fig. (**3**) as

$$x=x \quad , \quad y=u\cos\theta \quad , \quad z=u\sin\theta+v \quad \text{(A-2)}$$

then (A-1) becomes

$$\frac{\partial^2\Phi}{\partial x^2}+\frac{1}{\cos^2\theta}\left(\frac{\partial^2\Phi}{\partial u^2}-2\sin\theta\frac{\partial^2\Phi}{\partial u\,\partial v}+\frac{\partial^2\Phi}{\partial v^2}\right)=\frac{1}{c^2}\frac{\partial^2\Phi}{\partial t^2} \quad \text{(A-3)}$$

Let $\Phi = \sqrt{2}\phi \exp(j\omega t)$ then (A-1) can be given as

$$\frac{\partial^2 \phi}{\partial x^2} + \frac{1}{\cos^2\theta}\left(\frac{\partial^2 \phi}{\partial u^2} - 2\sin\theta \frac{\partial^2 \phi}{\partial u\,\partial v} + \frac{\partial^2 \phi}{\partial v^2}\right) + k^2\phi = 0 \qquad \text{(A-4)}$$

Let $V_x = -\partial\phi\ /\partial x$, $V_u = -\partial\phi\ /\partial u$ and $V_v = -\partial\phi\ /\partial v$ are the velocity component in the *x*, *u* and *v* directions, respectively. Assuming the walls of the cavity to be perfectly rigid and the loss at the wall can be neglected, the boundary conditions are

[1] at $x = 0,\ V_x = 0$ (A-5)

[2] at $x = a,\ V_x = 0$ (A-6)

[3] at $u = 0,\ V_u = 0$ (A-7)

[4] at $u = b$, $V_u = 0$ (A-8)

[5] at $v = 0,\ V_v = V_0\ F_0(x,u)$ (A-9)

[6] at $v = L$, $V_v = V_L\ F_L(x, u)$ (A-10)

where V_0 and V_L are the driving velocity at the input and output, $F_0(x,u)=1$ at the input and $F_0(x,u)=0$ elsewhere, $F_L(x, u)=1$ at the output and $F_L(x, u)=0$ elsewhere.

REFERENCES

[1] Nishimura Y, Nishimura S, Nishimura T, Yano T. Sound propagation in soundproofing casement windows. Appl Acoust 2009; 70: 1160-7.

[2] Ih JG. The reactive attenuation of rectangular plenum chambers. J Sound Vib 1992; 157 (1): 93-122.

[3] Eriksson LJ. Higher order mode effects in circular ducts and expansion chambers. J Acoust Soc Am 1980; 68(2): 545-50.

[4] Zander H. Active control of higher order acousticmodes in ducts. J Acoust Soc Am 1992; 92(1): 244-57.

[5] Yin Y, Horoshenkov KV. The attenuation of the higher-order cross-section modes in a duct with a thin porous layer. J Acoust Soc Am 2005; 117 (2): 528-35.

[6] Munjal ML. Acoustics of Ducts and Mufflers. New York: Willey 1987.

Received: January 4, 2012 Revised: February 23, 2012 Accepted: February 23, 2012

© Nguyen *et al.*; Licensee *Bentham Open*.

This is an open access article licensed under the terms of the Creative Commons Attribution Non-Commercial License (http: //creativecommons.org/licenses/by-nc/3.0/) which permits unrestricted, non-commercial use, distribution and reproduction in any medium, provided the work is properly cited.